CSIRO PUBLISHING

www.publish.csiro.au/journals/ijwf *International Journal of Wildland Fire*, 2005, **14**, 343–354

Spatial distribution and properties of ash and thermally altered soils after high-severity forest fire, southern California

Brett R. Goforth[A], *Robert C. Graham*[B,E], *Kenneth R. Hubbert*[C], *C. William Zanner*[D] *and Richard A. Minnich*[A]

[A]Department of Earth Sciences, University of California, Riverside, CA 92521, USA.
[B]Soil and Water Sciences Program, Department of Environmental Sciences, University of California, Riverside, CA 92521, USA.
[C]USDA Forest Service, Pacific Southwest Research Station, Forest Fire Laboratory, Riverside, CA 92507, USA.
[D]Department of Soil, Water, and Climate, University of Minnesota, Saint Paul, MN 55108, USA.
[E]Corresponding author. Telephone: +1 951 827 3751; fax: +1 951 827 3993; email: robert.graham@ucr.edu

Abstract. After a century of fire suppression, dense forests in California have fueled high-severity fires. We surveyed mixed conifer forest with 995–1178 trees ha^{-1} (stems > 10 cm diameter at breast height), and nearby pine–oak woodland having 175–230 trees ha^{-1}, 51 days after a severe burn, to contrast the spatial extent and properties of thermally altered soil at sites with different tree densities. Water-repellent soils were more extensive in forest than woodland. Deposits of white ash, composed largely of calicite, covered at most ~25% of the land surface, in places where large fuel items (e.g. logs, branches, exfoliated oak bark) had thoroughly combusted. At least 1690 kg ha^{-1} of $CaCO_3$ in ash was deposited over the forest, and at least 700 kg ha^{-1} was added to the woodland. Combustion of logs and large branches also reddened the underlying yellow-brown soil as deep as 60 mm (average 8 mm), and over ~1–12% of the land surface. The reddened soils have magnetic susceptibilities that are three to seven times greater than surrounding unreddened soils within the burn, indicating thermal production of maghemite. Such fire-altered conditions persist over spatial and temporal scales that influence soil genesis in Mediterranean-type climate regions.

Additional keywords: hydrophobic soil; maghemite; mixed conifer forest; reddened soil; soil magnetic susceptibility; soil pH; soil rubification; water-repellent soil; wood ash.

Introduction

Prior to fire suppression management, recurrent fires in the mixed conifer forests of southern California burned fallen leaf litter and woody stems while fatally scorching low-crown stature trees (Minnich 1988). This maintained low tree densities (<140 trees ha^{-1}, stems > 10 cm diameter at breast height (dbh)) with discontinuous canopy cover composed dominantly of large-diameter shade-intolerant pines (Minnich *et al*. 1995). Over the past century, forest fires have been extinguished as soon as possible to mitigate watershed sediment yield into reservoirs and to protect urban areas that interface with these wildlands (Kinney 1887). Because the thinning effect of recurrent fires has been largely eliminated by this fire suppression, present forests are dense (>250 trees ha^{-1}) with closure of canopy from below by shade-tolerant conifers (Minnich *et al*. 1995; Stephenson and Calcarone 1999). Deferred burning over extensive areas of forest has also resulted in accumulation of forest detritus (e.g. Albright 1998), because the prolonged warm-season drought characteristic of the Mediterranean-type climate in this region inhibits biological decomposition of fallen leaf litter and woody stems (Stohlgren 1988; Hart *et al*. 1992).

The available historical data indicate that burn intensities were heterogeneous over this forest landscape, moderated by low tree densities and discontinuous fuel loads within a mosaic of patches having burned at different times during a variety of fire weather conditions (Minnich 1987, 1988). Until recently, very little of the forest area had burned during the past century because prevailing fire weather conditions favor rapid extinguishment of ignitions. An indication of this is the contrast between average fire-return intervals (i.e. average time between fires for an area) before fire suppression that spanned decades of time, and intervals calculated from the present rate of burning, which have lengthened to centuries

 10.1071/WF05038 1049-8001/05/040343

(Minnich 1999). Currently, the greatest forest area is burned by a few large fires that coincide with brief periods of weather that make fire suppression most difficult (e.g. during warm, dry Foehn-type Santa Ana winds), as with adjoining chaparral (Minnich and Chou 1997). For example, forest and woodland were burned throughout the Cuyamaca Mountains in southern California during a Santa Ana wind event in October 2003. Few individual conifer trees survived the crownfire, and surface soil properties were conspicuously altered. The land surface was covered with thick deposits of white and dark ash, as well as patches of reddened mineral soil that contrasted with the yellow-brown hue of surrounding soils within the burned area.

The alteration of soil properties by fire has been investigated in recently burned forests and in laboratory experiments. White ash from thoroughly combusted pinewood has been studied to determine its composition (Etiegni and Campbell 1991) and relation to changes in soil pH and carbonate content (Ulery *et al*. 1993), as well as its role in clay dispersion (Durgin and Vogelsang 1984). Wildfires influence soil carbon and nitrogen dynamics as well as microbial communities (see in this issue: D'Ascoli *et al.* 2005; De Marco *et al.* 2005; Guerrero *et al.* 2005). Direct heating effects on mineral soil properties include changes in morphology (e.g. Sertsu and Sanchez 1978; Ulery and Graham 1993; Ketterings and Bigham 2000; Arocena and Opio 2003) and water repellency (e.g. DeBano 1981, 2000; Giovannini and Lucchesi 1983; Doerr *et al*. 1998, 2000), as well as alteration of clay and iron oxide minerals (e.g. Schwertmann and Taylor 1989; Ulery *et al*. 1996; Ketterings *et al*. 2000) with resultant changes in soil color (e.g. Ulery and Graham 1993; Ketterings and Bigham 2000) and magnetic properties (e.g. Ketterings *et al*. 2000). However, spatial assessment of ash and thermally altered soil properties has been lacking. Our study objectives were to: (1) contrast the spatial extent and properties of ash and thermally altered soil among a dense mixed conifer forest and a contiguous pine–oak woodland with lower tree density; (2) evaluate how thermally altered soil properties vary in relation to two differing parent material lithologies; and (3) to interpret the pedogenic implications of these fire-altered surface conditions in a Mediterranean-type climate.

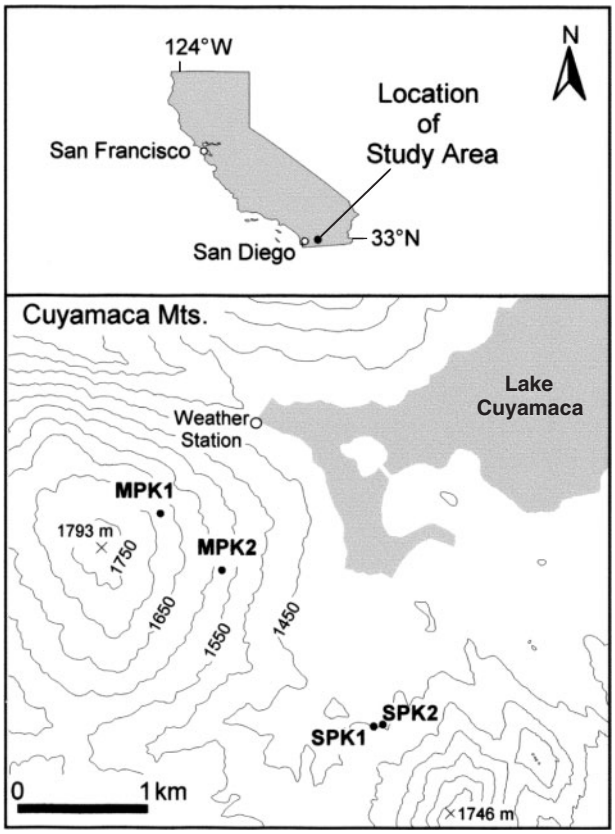

Fig. 1. Location of Middle Peak (MPK1, MPK2) and Stonewall Peak (SPK1, SPK2) study sites in the Cuyamaca Mountains, southern California.

Materials and methods

Study area

Severely burned forest was located in the Cuyamaca Mountains, ~60 km east of San Diego, California (Fig. 1). We examined soils at two areas with differing lithology and tree density, referred to as Middle Peak and Stonewall Peak. Fire history maps indicate that no previous burning had occurred in these areas since government record keeping began in year 1911, although pre-historical burns were evident from fire-scars observed on large trees. At the time of study, both areas exhibited complete canopy-scorched defoliation of trees due to crownfire, while the land surface lacked residual unburned leaf litter and woody debris smaller than 2.5 cm in diameter. Aerial photograph analysis and ground surveys indicated that crownfire was prevalent over nearly the entire surrounding forest and woodland (ca. 10 000 ha). The Cuyamaca Mountains are uplifted Cretaceous intrusive-igneous batholith rock within the broader Peninsular Range. Soils are locally derived from gabbro colluvium at Middle Peak, and granodiorite colluvium at Stonewall Peak. Soils have been classified as fine-loamy, mixed, mesic Ultic Haploxeralfs at Middle Peak and coarse-loamy, mixed, mesic Ultic Haploxeralfs at Stonewall Peak (Soil Survey Staff 1999). The A horizons of soils at both locations have sandy-loam to loam textures. A nearby weather station at the Lake Cuyamaca Dam (Fig. 1) indicates a montane Mediterranean-type climate with cold, wet winters and warm, dry summers. Annual precipitation totals averaged 932 ± 351 mm (standard deviation) over the period 1887–2001, and 87% of the annual total accumulated during November–April winter storms. Approximately 15% of annual precipitation at the elevation of our study area was snowfall (Minnich 1986). The annual average temperature is 11.6°C, with monthly average temperatures between 4°C (January) and 21°C (July). Vegetation distributions in

Table 1. Description of study sites at Middle Peak and Stonewall Peak
AC, *Abies concolor*; CD, *Calocedrus decurrens*; dbh, diameter at breast height (1.3 m height from surface on uphill side); PJ, *Pinus jeffreyi*; PL, *Pinus lambertiana*; QC, *Quercus chrysolepis*; QK, *Quercus kelloggii*

Site[A]	Location	Elevation (m)	Aspect	Slope (%)	Tree density (ha^{-1})[B]		Basal area ($m^2\ ha^{-1}$)		Species composition (%)
					All stems	>10 cm dbh	All stems	>10 cm dbh	
MPK1	32°58.9′N, 116°35.9′W	1670	N	11	1600	995	80.00	77.54	CD, 34; AC, 25; QC, 23; PL, 17; QK, 1
MPK2	32°58.8′N, 116°35.4′W	1585	E	23	1680	1178	56.17	53.83	CD, 73; QC, 25; QK, 2
SPK1	32°58.1′N, 116°34.5′W	1445	N	24	207	175	23.27	23.14	PJ, 50; QK, 35; QC, 15
SPK2	32°58.2′N, 116°34.4′W	1450	N	19	270	230	36.02	35.92	PJ, 57; QK, 43

[A]MPK1 and MPK2 soil is derived from gabbro colluvium, and classified as fine-loamy, mixed, mesic Ultic Haploxeralfs; SPK1 and SPK2 soil is derived from granodiorite colluvium, and classified as coarse-loamy, mixed, mesic Ultic Haploxeralfs.
[B]Oak trees (*Quercus* spp.) often had multiple stems with canopy stature that branched below a height of 1.3 m (dbh) from a common root crown base. Each of these stems was counted separately and measured. Trees with branching at dbh, or above dbh, were counted as a single stem and measured.

this region correlate with the patterning of annual precipitation and evapotranspiration along gradients of elevation, slope aspect and topographic position (e.g. Stephenson 1998; Minnich and Everett 2001). Forests and woodlands are most prevalent on relatively mesic polar-facing slope aspects in the study area. A mixed conifer forest consisting of white fir (*Abies concolor*), incense cedar (*Calocedrus decurrens*), sugar pine (*Pinus lambertiana*), ponderosa pine (*P. ponderosa*), canyon live oak (*Quercus chrysolepis*) and California black oak (*Q. kelloggii*) occurred at Middle Peak, with 995–1178 trees ha^{-1} (stems > 10 cm dbh; Table 1). A pine–oak woodland with Jeffrey pine (*P. jeffreyi*), canyon live oak and California black oak occurred at Stonewall Peak, with 175–230 trees ha^{-1}. Fieldwork was conducted 51 days after the fire, a period that registered 66 mm of precipitation at Lake Cuyamaca Dam.

Field measurements

We used line-intercept transects to survey the spatial distribution and properties of ash and thermally altered soils within the burn. Two transect origins were established in pine–oak woodland at Stonewall Peak (SPK1, SPK2) and mixed conifer forest at Middle Peak (MPK1, MPK2), located within 0.5 km of roads to minimize the hauling distance of sample materials. Our selection of these four locations was purposive because we avoided sampling where the land surface had been disturbed after fire, or in places where it was mostly exposed rock. Three transects were surveyed from each origin. We selected a random azimuth heading for the first transect using a calculator number generator, and the remaining two transects were separated by 120°. Transects were 44 m long at MPK1 and SPK1, and 24 m long at MPK2 and SPK2.

Observations and soil collections started at 4 m from the origin to avoid surface disturbance caused by our establishment of each transect. We tested for carbonate abundance in ash deposited over the land surface by observing the production of effervescent foam in reaction to droplets of 1 M HCl solution applied at 1-m intervals along each transect (Schoeneberger *et al*. 2002). Ash and charred O horizon materials were collected at effervescence test locations for laboratory analysis, as were underlying soil samples at the 0–2-cm and 2–5-cm depths. At each transect intersection with a patch of reddened soil, we measured the transect interval that crossed over the patch, and the maximum depth of reddening. The contributing combustion feature was recorded (e.g. branch, log, stump), and samples of reddened soil material were collected for laboratory analysis. While no parts of the landscape at Middle Peak and Stonewall Peak were unburned, we attempted to find soils that were less severely affected by the fire for comparison. These samples were collected along the transects in places where the surface was not apparently reddened or covered with white ash, at the 0–2-cm and 2–5-cm depths of the soil profile (henceforth 'profile soils'). Known volumes for bulk density measurements were collected from profile soils using a metal cylinder of 7.3-cm diameter and 5.1-cm length to extract cores where feasible. For thinner layers of ash and reddened soil, intact material was carved into small blocks in place, the dimensions were measured, and the known volume of material was collected. We evaluated the water repellency of soils within the burn by observing the water drop penetration time (WDPT) of 10 droplets applied over a 6 × 6 cm area at the soil surface, the 2-cm depth and the 4-cm depth. These WDPT test locations were spaced at 8-m intervals along our first transect at MPK1, although subsequently at 4-m intervals along all other transects for more intensive sampling. We qualitatively observed the field moisture condition at each WDPT test location (moist, dry, intermediate), and recorded the time of complete droplet absorption within four categories: 0–5, 5–30, 30–180 and >180 s. Bulk soil samples were collected to determine gravimetric moisture content among the field moisture conditions observed at WDPT test locations. After the survey of ash and soils was completed, tree densities were measured over a 0.125-ha area encircling the transect origin. Basal area was totaled within this plot after measuring each stem dbh (= 1.3 m height from surface on uphill side), and the data are reported by ha^{-1} equivalency in Table 1.

Laboratory procedures

All samples were air-dried in a low-humidity environment (<30% relative humidity (RH)) and sieved into <2 mm and >2 mm fractions. Bulk density values were corrected for the >2 mm fraction volume and weight (Soil Conservation Service 1984). Color was measured on air-dried samples using a chromameter (Model CR-200, Minolta Corporation, Ramsey, NJ, USA), and the average of three measurements was expressed using both the Munsell and International Commission on Illumination (CIE) notations (Torrent and Barrón 1993). The pH of soil, and most ash samples, was measured on a 1 : 1 sample : water ratio. A few ash samples needed a 2 : 1 ratio in order to produce a slurry suitable for pH measurement. An ancillary study showed that the different sample : water ratio changed the pH by no more than ±0.1 pH unit. This small variation was disregarded for subsequent data analysis. Total carbon and nitrogen were determined by dry combustion using a C/N analyser (Nelson and Sommers 1996). Calcium carbonate equivalent (CCE) was measured using a manometric method for 0.3 g samples over 1 h duration (Loeppert and Suarez 1996). Organic carbon was calculated by subtracting the inorganic carbon contributed by the calcium carbonate from the total carbon. Magnetic susceptibility, the ratio of the magnetization of a sample to the magnetic field inducing the magnetization (Mullins 1977), was measured with a Bartington MS2B dual frequency magnetic susceptibility meter (Bartington Instruments, Oxford, UK). Air-dried samples of the <2 mm sieved fraction with known mass were contained in 10-mL sample cubes, and the average of three magnetic susceptibility measurements was recorded for each sample at low (0.46 kHz) and high (4.6 kHz) sensor frequencies. Low-field mass-specific magnetic susceptibility (χlf) was calculated as the average low-frequency measurement divided by the sample density, and frequency-dependent low-field susceptibility (χfd) was calculated as the percentage loss of mass-specific susceptibility (Evans and Heller 2003). White ash samples collected within the burn were analysed by X-ray diffraction (XRD) of dry packed powder mounts using CuKα radiation and a graphite crystal monochromator. The pattern of XRD peaks was inventoried by step scanning at 1-s intervals per 0.02°2θ, from 2° to 65°2θ. The chemical and physical properties that we analysed for white ash, dark ash, reddened soil and profile soils are reported in Table 2.

Results and discussion

Heterogeneity of post-fire soil wettability

Field moisture conditions and water-repellent soils were spatially variable in both the dense forest and lower tree-density woodland. At the time of burning, the top 4 cm of the soil profile was likely dry as the most recent precipitation event preceded the fire by 53 days and amounted to only 4 mm of rainfall. By the time of our observation 51 days after the fire, 66 mm of precipitation had occurred, which is equivalent to 7% of the mean annual amount. Gravimetric moisture content ranged from 14 to 30% among bulk soil samples collected at the surface, 2-cm and 4-cm depths at forest and woodland sites. The WDPT significantly differed between forest and woodland sites at the soil surface (χ^2 test, $\alpha = 0.05$, d.f. $= 2$, $\chi^2 = 12.6$, $P = 0.002$), as well as the 2-cm soil depth (d.f. $= 2$, $\chi^2 = 216.0$, $P = 0.000$) and the 4-cm soil depth (d.f. $= 2$, $\chi^2 = 200.7$, $P = 0.000$). Water-repellent soils were more extensive in dense forest at Middle Peak than in woodland at Stonewall Peak where the average tree density was five times less (Table 1; Fig. 2), despite similar soil texture in the A horizon among sites.

Biological decomposition of humified organic matter produces compounds that cause water repellency in unburned surface soil horizons (e.g. Bisdom *et al*. 1993). These organic compounds volatize in surface soils exposed to heating intensities of ~250°C over a period of several minutes, and a portion of this vapor adsorbs to cooler soil particle surfaces at depth to form a horizon with diminished wettability (Savage *et al*. 1972; Savage 1974; DeBano *et al*. 1976; DeBano 1981). The depth and thickness of this water-repellent layer is dependent on antecedent properties that affect heat penetration into soil (e.g. soil texture, field moisture conditions), as well as the surface combustion intensity and the duration of soil heating (DeBano 2000; Doerr *et al*. 2000). Soil water repellency is eliminated by prolonged heating that exceeds the ~280°C combustion temperature of the volatized organic compounds that cause water repellency (e.g. DeBano *et al*. 1976; Doerr *et al*. 2004). Combustion intensities were apparently sufficient to eliminate water-repellent compounds over most of the soil surface, as indicated by the trend of decreasing soil wettability with depth in the profile (Fig. 2). Water-repellent profile soils were more extensive in dense forest at Middle Peak than in the lower tree-density woodland at Stonewall Peak, likely due to more abundant accumulation of soil organic matter requisite for the volatilization and translocation of water-repellent compounds.

Properties and spatial distribution of ash

Most of the land surface in the study area was covered with deposits of dark and white colored ash. The white ash had significantly higher Munsell hue, value and chroma, as well as color lightness (CIE L*) compared to the dark ash (Table 2). We did not measure the spatial distribution of white and dark ash directly because there was often a fine-scale heterogeneity of the two types. However, only the white ash would vigorously react to droplets of 1 M HCl solution, producing an effervescent foam represented by the 'violent effervescence' category in Fig. 3 that was observed among 1–25% of all test locations in the study area. Variations among categories of effervescence observed over the land surface are dependent on site (χ^2 test, $\alpha = 0.05$, $\chi^2 = 118.6$, d.f. $= 12$, $P = 0.000$). The combined proportion of strong and violent effervescence

Table 2. Selected physical and chemical properties of ash and soil samples

Reported data are averages for *n* samples analyzed within each ash and soil category. Data within columns followed by the same superscript letter did not differ significantly using Duncan's multiple-range test ($\alpha = 0.05$). All results are for <2 mm particle size fraction. CCE, $CaCO_3$ equivalent; OC, organic C; RR, redness rating

Site	Sample material	*n*	Dry color[A]					pH	CCE ($g\,kg^{-1}$)	N ($g\,kg^{-1}$)	OC ($g\,kg^{-1}$)[B]	OC : N	Bulk density[C]		Magnetic susceptibility[D]		
			Hue	Value/chroma	RR	CIE L*	CIE a*						*n*	$g\,cm^{-3}$	*n*	χlf ($\times 10^{-8}\ m^3\,kg^{-1}$)	χfd (%)
Middle Peak	White ash	5	3.0Y	4.7/1.5	–	53.63^{b}	0.24^{d}	10.1^{b}	642.1^{b}	$0.6^{c,d}$	6.9^{c}	$12^{a,b,c}$	3	0.18	4	706.80	6.9
	Dark ash	19	0.8Y	3.0/0.9	–	33.82^{e}	1.22^{d}	8.0^{d}	70.5^{c}	$3.1^{a,b}$	$48.3^{a,b}$	$15^{a,b}$	2	0.30	7	1265.80	6.9
	Reddened soil	8	7.2YR	4.4/3.6	3.3	44.47^{c}	9.30^{a}	$8.3^{c,d}$	21.8^{d}	$0.3^{c,d}$	3.8^{c}	$10^{b,c}$	3	0.55	5	2342.54	6.5
	Soil profile												3	0.69			
	0–2 cm	6	8.3YR	3.0/1.7	1.0	31.04^{e}	$4.05^{b,c}$	7.2^{e}	13.7^{d}	$3.4^{a,b}$	$44.9^{a,b}$	$13^{a,b}$			2	739.30	5.3
	2–5 cm	6	7.5YR	3.3/2.3	1.7	33.85^{e}	5.93^{b}	$6.6^{e,f}$	8.0^{d}	$3.0^{a,b}$	$46.0^{a,b}$	15^{a}			1	834.50	5.6
Stonewall Peak	White ash	3	8.4Y	6.9/1.0	–	70.61^{a}	-0.75^{d}	11.7^{a}	858.0^{a}	$0.4^{c,d}$	3.9^{c}	$12^{a,b,c}$	2	0.45	1	79.30	9.3
	Dark ash	19	0.6Y	3.1/0.7	–	32.13^{e}	1.04^{d}	8.1^{d}	$41.4^{c,d}$	4.2^{a}	66.3^{a}	$15^{a,b}$	2	0.37	2	195.40	7.5
	Reddened soil	8	6.9YR	4.5/3.2	2.2	45.52^{c}	8.25^{a}	8.9^{c}	20.5^{d}	0.2^{d}	1.4^{c}	8^{c}	2	0.77	4	548.75	8.4
	Soil profile												3	0.85			
	0–2 cm	7	9.8YR	3.8/2.1	0.2	39.73^{d}	3.44^{c}	6.6^{f}	8.5^{d}	$2.1^{b,c}$	$34.0^{a,b,c}$	17^{a}			3	73.47	5.9
	2–5 cm	7	9.9YR	3.8/2.1	0.2	38.68^{d}	3.49^{c}	6.5^{f}	8.6^{d}	$1.6^{b,c,d}$	$26.8^{b,c}$	16^{a}			3	82.80	6.6

[A] RR = [(10 − YR hue) × chroma]/value; CIE L* = lightness; CIE positive a* = redness; higher CIE coordinates indicate greater color property.

[B] OC = Total C% − (CCE% × 0.12).

[C] Bulk densities reported for profile soils were determined from cylindrical cores of soil material collected through the 0–5 cm depth.

[D] Low-field (0.46 kHz) mass-specific magnetic susceptibility (χlf), and frequency-dependent low-field susceptibility (χfd).

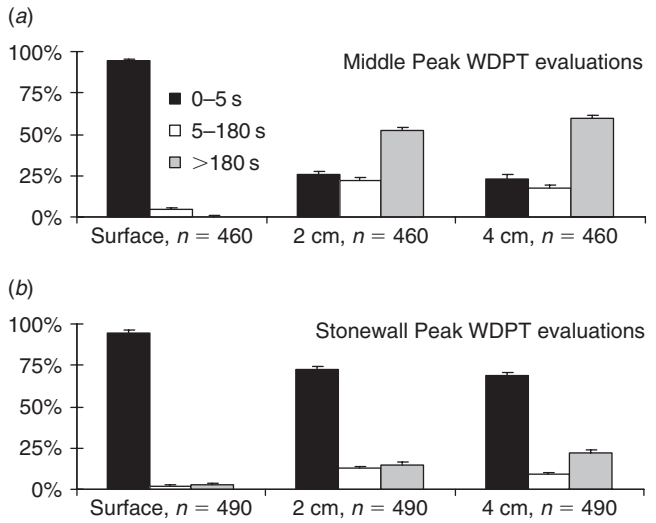

Fig. 2. Percentages of water drop penetration time (WDPT) categories observed in (*a*) dense forest and (*b*) lower tree-density woodland at the soil surface, 2-cm soil depth and 4-cm soil depth. Error bars indicate the range of 1 standard error for each proportion.

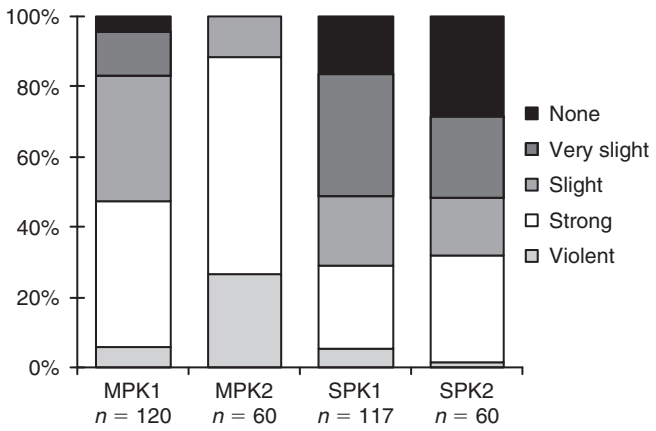

Fig. 3. Percentages of field effervescence categories observed over the land surface along transects at each site. Three test locations at SPK1 were over exposed rock, and are omitted from the analysis.

was greatest in dense forest sites (~50–90% of test locations), compared with woodland sites (only ~30% of test locations). Some effervescence was observed at all test locations along transects in the most dense forest we surveyed (MPK2), while ~15–30% of the land surface at the woodland sites lacked effervescence (Fig. 3). Concentrations of white ash, 3–4 cm thick, were observed where large woody fuel items (e.g. logs, branches) had combusted, as well as around the base of some standing oak trees where exfoliated bark had burned.

Residual organic C is a darkening pigment in ash. The color lightness of ash can therefore indicate whether combustion of organic matter is incomplete or more thorough. The average CIE L* coordinate of white ash in a pooled analysis was 60.00 ± 10.90 compared to an average of 32.97 ± 3.68 for pooled dark ash. We found that variation in color lightness of ash was correlated with variation in pH ($r^2 = 0.887$), CCE ($r^2 = 0.822$), total N ($r^2 = 0.744$), and total organic C ($r^2 = 0.722$). Both pH and CCE increased with lighter ash color, while total N and organic C content increased with darker ash color (Fig. 4). Dark ash is a product of incomplete combustion, as indicated by its higher organic C content compared to the white ash (Table 2).

The elemental composition of ash may vary according to plant material (e.g. stem, bark, leaf) and plant species. Ashes produced from the combusted leaf litter of conifer and oak species that occurred in the study area contain Ca, K and Mg (St John and Rundel 1976). Calcium is most abundant in white ash produced from pine wood and oak wood, as well as from oak bark (Etiegni and Campbell 1991; Ulery *et al.* 1993). Complete combustion of these fuels at temperatures near 500°C produces a light gray or white-colored ash composed of alkaline earth oxides (Ca, K and Mg oxides), that over time react with atmospheric CO_2 and water vapor to form soluble hydroxides and carbonates (Etiegni and Campbell 1991; Ulery *et al.* 1993).

The average CCE of white ash in this study was 9–20 times greater than surrounding dark ash, indicating more abundance of alkaline earth oxides initially available to form carbonates after the fire. The XRD pattern for a white ash sample with pH of 12.6 (Fig. 5) shows high-intensity peaks for calcite ($CaCO_3$) and low-intensity peaks for calcium oxide (CaO). In contrast, XRD did not detect calcium oxide in a less alkaline white ash sample in which $CaCO_3$ was also abundant (Fig. 5), though the pH of 8.8 for this sample was higher than that expected if $CaCO_3$ content had attained equilibrium with atmospheric CO_2 (pH ~8.3). The XRD pattern for white ash samples also included low-intensity peaks for quartz (SiO_2), feldspars (not labeled) and phyllosilicates (not shown). We observed that the white ash was contaminated with surrounding soil materials, perhaps by rain drop impacts and aeolian deposition during the 51 days after fire (Ulery *et al.* 1993).

We estimated the minimum amount of calcium carbonate ($CaCO_3$) deposited over the land surface from this forest fire. First, the area of ash coverage per hectare at each site was estimated from the effervescent portion of the land surface observed along our transects (Fig. 3). Then we calculated the average volume of ash per hectare at each site using the average ash thickness at Middle Peak (8 ± 4 mm standard deviation) and Stonewall Peak (6 ± 3 mm) as measured along our transects. Data for dark ash bulk density at each site were used to correct these ash volumes, since dark ash was much more extensive than the deposits of white ash, though lower in CCE (Table 2). The amount of $CaCO_3$ contained in each corrected ash volume was determined using the CCE for dark ash at each site. A minimum of 1690 kg ha^{-1} of $CaCO_3$ in ash was added to the land surface in dense forests at Middle

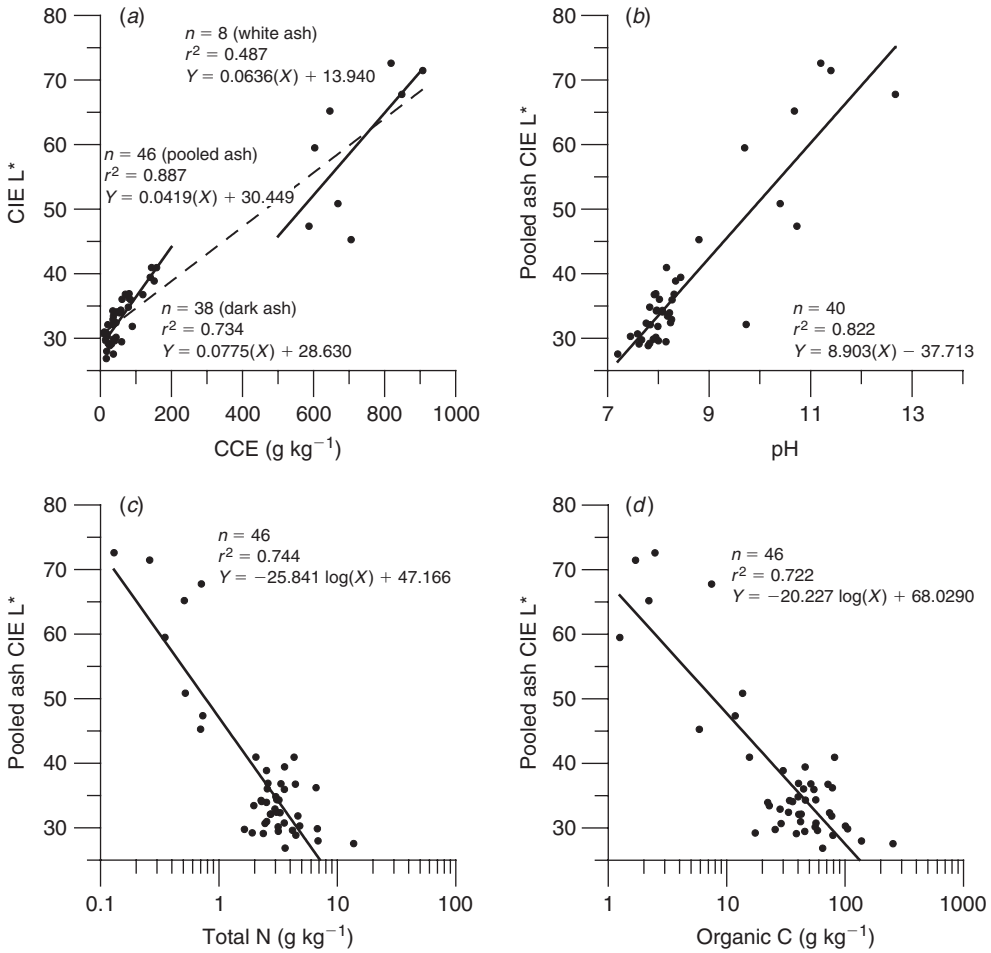

Fig. 4. Linear regression of color lightness (CIE L*) with selected chemical properties of ash. (*a*) $CaCO_3$ equivalent (CCE); (*b*) pH; (*c*) total nitrogen; and (*d*) organic carbon.

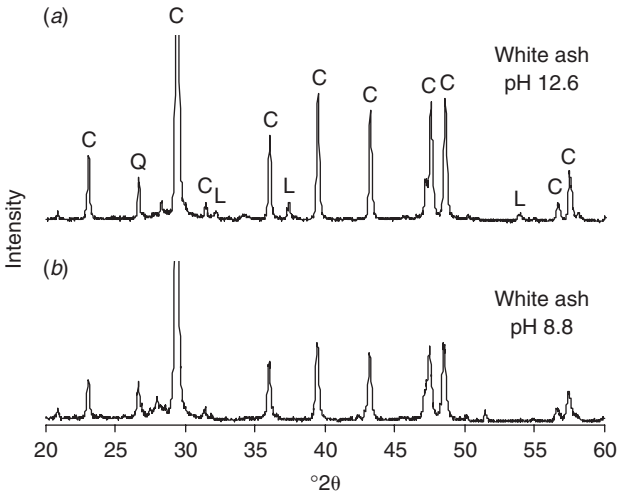

Fig. 5. XRD pattern for dry packed-powder mounts of white ash with pH (*a*) 12.6 and (*b*) 8.8. Identified peaks are for calicite (C; $d = 0.386$, 0.3035, 0.284, 0.249, 0.228, 0.209, 0.191, 0.187, 0.162, 0.160 nm), calcium oxide (L; $d = 0.278$, 0.2405, 0.170 nm), and quartz (Q; $d = 0.3343$ nm).

Peak, and at least 700 kg ha^{-1} of $CaCO_3$ was added to the lower tree-density woodland at Stonewall Peak.

Properties and spatial distribution of reddened soils

In addition to white ash, patches of reddened soil were visually prominent at both study sites. The pattern of reddening consisted of linear stripe-like patches over the land surface where logs had burned (Fig. 6), and irregular subsurface masses of reddened soil surrounding cavities where stumps and roots had combusted. Samples of this reddened soil material have calculated redness ratings (Torrent *et al*. 1983) that are 3–11 times greater than surrounding profile soils within the burn, which have yellow-brown hues. The color lightness and redness (CIE positive a*) of the severely burned soil material did not significantly differ between sites regardless of parent material lithology (Table 2). Profile soils at Middle Peak, derived from gabbro colluvium, are significantly darker (lower CIE L*) than profile soils derived from granodiorite colluvium at Stonewall Peak (Table 2). The chemical properties we analysed for reddened soil materials

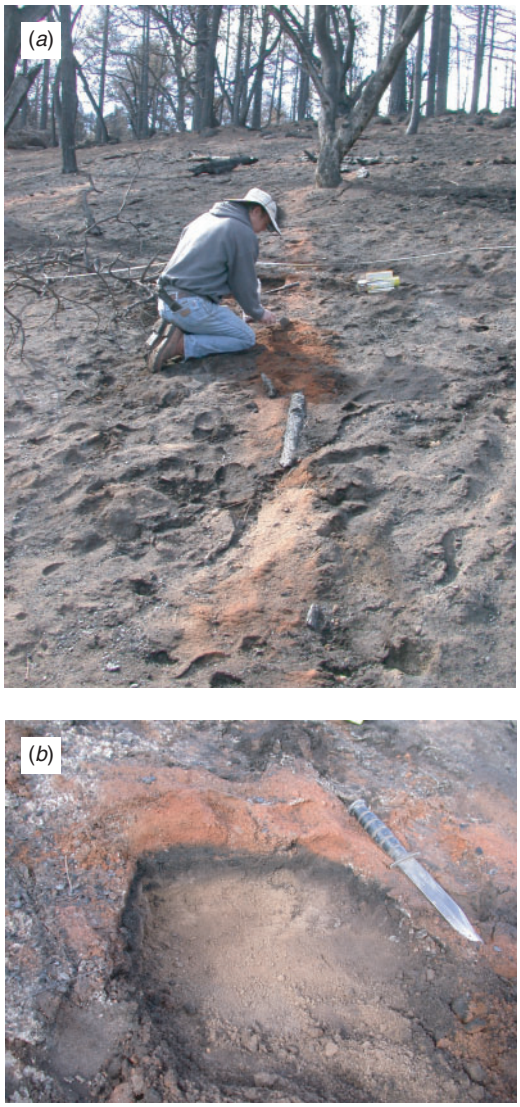

Fig. 6. (*a*) Linear patches of exposed reddened soil material occurred over the land surface where logs had thoroughly combusted. (*b*) When observed in cross-section profile, reddened mineral soil was underlain by a charred, darkened zone, and unaltered soil material at lower depth. Soil knife indicates 30 cm for scale.

(pH, CCE, total N, organic C, OC : N) did not differ significantly between sites despite contrasting parent material lithology and tree density (Table 2). Differences in CCE were not significant between the reddened soil material and profile soils because an extensive coverage of ash at both Middle Peak and Stonewall Peak sites resulted in significant input of $CaCO_3$ within the solum, perhaps due to illuviation caused by 66 mm of precipitation after fire. The lowest amounts of nitrogen and organic carbon detected in this study were among the surface patches of reddened soil (Table 2), indicating near-complete combustion of soil organic matter.

Surface patches of reddened soil material had a detectible increase in magnetization compared to surrounding soils within the burned area. Reddened soil materials collected from both Middle Peak and Stonewall Peak sites have low-field mass-specific magnetic susceptibility (χlf) measurements that are three to seven times greater than 0–2-cm-depth profile soils having yellow-brown hues (Table 2). While the χlf of reddened and profile soils was greatest at sites with mafic lithology at Middle Peak, reddened soils derived from the more felsic parent material at Stonewall Peak had a larger increase in χlf compared to the 0–2-cm-depth profile soils. Bulk density of the reddened soil materials was on average less than that of the profile soils, but greater than that of white and dark ash at both sites. Yet, the change in χlf between reddened soil materials and surrounding profile soils exceeds that expected to result from a simple reduction in bulk density caused by the combustion of soil organic matter. Differences in frequency-dependent low-field susceptibility (χfd) between reddened soil material and 0–2-cm-depth profile soils at Middle Peak and Stonewall Peak suggest that there was an increase in fine-grained ferrimagnet content in the soil reddened by severe burning (Dearing 1994).

The red color of severely burned soil material is imparted by maghemite (γ-Fe_2O_3) and hematite (α-Fe_2O_3). When soil is heated at 300–500°C, its content of goethite (α-FeOOH) transforms to hematite and more abundantly to maghemite if in the presence of combusting soil organic matter that results in an oxygen-deficient environment (Schwertmann and Fechter 1984; Schwertmann 1988; Schwertmann and Taylor 1989). The precursor mineral goethite, a yellow-brown iron oxyhydroxide, is a common weathering product of mafic minerals in well-drained soils (Schwertmann and Taylor 1989; Bigham *et al*. 2002) as found at our study sites. The yellow-brown color of our profile soil samples is consistent with the hue, value and chroma of soil material containing goethite, while reddened soil samples in this study match with maghemite or hematite (Schwertmann and Taylor 1989; Schwertmann 1993; Scheinost and Schwertmann 1999; Bigham *et al*. 2002). Hematite and maghemite have differing magnetic properties that are useful for identification (e.g. Mullins 1977). Hematite is the antiferromagnetic structure of Fe_2O_3, exhibiting a relatively weak magnetic susceptibility compared to maghemite with ferrimagnetic form (Mullins 1977; Schwertmann 1988). The increased χlf of reddened soil materials compared to surrounding profile soils (Table 2) indicates an abundant production of maghemite in these places where large woody fuels burned over long durations.

The greatest extent of reddened land surface was observed among dense forest sites (Middle Peak), ranging from 1 to 15% of the total land surface (Table 3). At woodland sites with lower tree density (Stonewall Peak), only ~1–5% of the land surface was reddened. The average thickness of reddened soil along all transects was 8 mm, though reddened soil materials were as much as 60 mm thick. Similar distributions of reddened soil material have been observed after fire elsewhere,

Table 3. Percentage of transect length reddened within sites

Transect	MPK1	MPK2	SPK1	SPK2
1	2.5	5.9	1.3	3.2
2	1.0	13.9	0.6	5.1
3	3.4	15.3	0.9	2.0
Average	2.3	11.7	0.9	3.4

in the places where logs burned on the land surface (e.g. Boyer and Dell 1980; Ulery and Graham 1993) and under burned piles of cut vegetation (e.g. Sertsu and Sanchez 1978; Ketterings and Bigham 2000). Because ~1–12% of the land surface was reddened in this study (Table 3), and the average thickness of reddened soil patches was 8 mm, we estimate 0.1–1 mm of reddened soil was produced from this single fire event, if evenly spread over the land surface.

Long-term implications

Ash can have a lasting influence on pH conditions over the land surface and in the solum. Soils in the study area typically do not contain carbonates and have moderately to slightly acidic pH (5.7–6.5), but in the post-fire environment, we detected 8–14 g kg^{-1} CCE in profile soils and neutral to moderately alkaline soil pH (6.6–8.2) at the dense forest site. In a study of burned areas in the mountains of California, Ulery *et al*. (1993) found that the pH of white ash decreased from 12.0 at a burned site 22 days after fire to 9.3 at a 60-day-old burn, as the calcium oxide (CaO) converted to less alkaline calcium carbonate. However, calcium carbonate produced by forest fires can persist for years, as Ulery *et al*. (1993) detected $CaCO_3$ in 3-year-old white ash with a pH of 7.8. We have observed the violent effervescence of white ash with 1M HCl solution over the past 5 years after the Manter Fire of year 2000 in the southern Sierra Nevada mountains of California. Dissolution of $CaCO_3$ in these residual deposits of white ash may alter the ion exchange properties of soil minerals with pH-dependent charge, and cause the dispersion of kaolinite, promoting illuviation within the solum and erosion over the land surface (Durgin and Vogelsang 1984; Ulery *et al*. 1993). Eventually, surface deposits of $CaCO_3$ are heterogeneously mixed into the A horizon by burrowing fauna, to persist as fragmental masses within the soil that maintain alkaline pH (7.4–8.0) until dissolved by percolating meteoric waters that leach the solum.

It is widely observed that well-drained soils, particularly in warm climate regions, become redder with time, a process referred to as rubification (Birkeland 1999). Hematite and maghemite are the main reddening pigments that remain stable within well-drained soils, and accumulate as other soil minerals weather (Singer *et al*. 1996; Bigham *et al*. 2002). Both hematite and maghemite are weathering products of mafic minerals inherited from parent materials (e.g. Schwertmann 1988; Fine *et al*. 1989; Schwertmann and Taylor 1989). Production of hematite and maghemite by recurrent fires is suggested to enhance the cumulative reddening of well-drained soil profiles in forests and woodlands with Mediterranean-type climates (e.g. Ulery and Graham 1993). Reddened soil material produced over a severely burned land surface can be mixed into the solum by processes of eluviation, tree throw and faunal burrowing, while combustion of tree stumps and large roots can directly redden subsurface soil materials (Stanjek 1987; Schwertmann 1993; Ulery and Graham 1993). Even if these pedoturbation processes efficiently dilute reddened soil materials within the solum, appreciable reddening may occur because hematite, and presumably maghemite, can impart red pigmentation in soils even if composing only 1% of the overall mineral content (e.g. Torrent *et al*. 1983).

The results of our study allow an assessment of potential soil reddening by past forest fires. We calibrated the reddened land surface area measured in our study with observations of fuel volumes in the Sierra San Pedro Mártir, a forest 250 km south in northern Baja California, Mexico. This forest has many of the same conifer species and similar environmental gradients, but had not been altered by fire suppression and tree harvesting activities when studied (Minnich *et al*. 2000). Aerial photographic surveys of the Sierra San Pedro Mártir detected logs (>30 cm diameter) at densities ranging from 2 to 6 ha^{-1}, with an average coverage equivalent to ~1% of the land surface (Minnich *et al*. 2000), or 13.64 tons ha^{-1} if all woody fuels >7.7-cm diameter are considered (Stephens 2004). This loading of large woody fuel items is consistent with the lower limit of reddened land surface measured in our study, as well as that suggested by Ulery and Graham (1993) in nearby forests and woodlands. We estimated the cumulative amount of soil reddening over a forest landscape caused by recurrent fires using our minimum observed reddened area (1% of surface), our average reddened soil thickness (8 mm), and an interval of 50 years between fires mapped from time-series aerial photography of the Sierra San Pedro Mártir (Minnich *et al*. 2000). During the Holocene (10 000 years), recurrent forest fires may have cumulatively produced at least 16 mm of reddened soil over the landscape. If we calculate back into the Pleistocene, say over the past 50 000 years, it is expected that 80 mm of reddened soil was produced. These reddened soil materials are mixed into the solum by pedoturbation processes over time, while burned roots and stumps may additionally redden soil beneath the land surface. Though such long-term estimates are subject to uncertainties regarding climatic and vegetation changes, they suggest that forest fires are a contributing influence to the rubification of well-drained soils in this Mediterranean-type climate region. Studies that document this trend in southern California (e.g. McFadden and Hendricks 1985; McFadden and Weldon 1987; Harden and Matti 1989; Kendrick and McFadden 1996) were conducted

at elevations perhaps covered by forest or woodland in the past 50 000 years during moister glacial climate, though these areas are now shrublands that lack the large woody fuels necessary to effectively burn and redden soils.

Conclusions

We contrasted the spatial extent and properties of ash and thermally altered soil after a recent high-severity fire within a dense mixed conifer forest and a contiguous pine–oak woodland where tree densities were on average five times less, and we evaluated how thermally altered soil varied among two different parent material lithologies. After receiving 66 mm of precipitation since the fire, water-repellent soils were more extensive in dense forest at Middle Peak than within woodland at Stonewall Peak, where tree density is lower. Combustion in the dense mixed conifer forest produced a more uniform abundance of alkaline earth oxides in ash that was available for the secondary production of $CaCO_3$, than was observed in the woodland. At least 1690 kg ha^{-1} of $CaCO_3$ were added to the dense forest, and at least 700 kg ha^{-1} of $CaCO_3$ were added to the less-dense woodland. The pH and CCE of ash increased with lighter color, while total N and organic C content increased with darker color. Reddened soil material occurred on the land surface as linear stripe-like patches in places where fallen trees had burned, as well as surrounding cavities within the solum where stumps and roots had combusted. This reddened soil had mass-specific magnetic susceptibilities that were three to seven times greater than surrounding unreddened soils within the burned area, indicating abundant content of thermally produced maghemite. Magnetic susceptibilities of reddened soils were greatest at sites with mafic lithology, though reddened soils derived from a more felsic parent material had a larger increase in susceptibility compared to surrounding unreddened soils within the burned area. While reddened soil was observed in both forest and woodland, the greatest area of reddened land surface was in the dense mixed conifer forest, presumably due to more abundant downed woody fuels.

Recurrent forest fires over thousands of years may significantly contribute to the cumulative reddening and magnetic susceptibility of well-drained soils in Mediterranean-type climate regions. As this study and others have shown (e.g. Ketterings *et al*. 2000), surface patches of reddened soil indicate the places where soil was severely burned and are detectible by a characteristic increase in magnetization compared to surrounding soil. Hence, the long-term patterning of forest fire intensities over a landscape may be detectable as the spatially heterogeneous accumulation of thermally produced iron oxides in soils.

Acknowledgements

This research was funded by California State Parks Interagency Agreement C0343027, with support of the University of California Agricultural Experiment Station at Riverside. We thank Jim Dice, Paul Jorgensen and Mathew Fuzie of California State Parks for permitting our research in Cuyamaca Rancho State Park, and Jamie Nichols for completing the laboratory measurements of color, pH, total carbon and nitrogen, and carbonates, and Paul Sternberg for assistance with XRD. Criticisms provided by three reviewers and Robert Goforth were helpful in revising this manuscript.

References

Albright D (1998) Vegetation change in second-growth mixed conifer forests of western San Bernardino Mountains. MS Thesis, University of California, Riverside.

Arocena JM, Opio C (2003) Prescribed fire-induced changes in properties of sub-boreal forest soils. *Geoderma* **113**, 1–16. doi:10.1016/S0016-7061(02)00312-9

Bigham JM, Fitzpatrick RW, Schulze DG (2002) Iron oxides. In 'Soil mineralogy with environmental applications'. (Eds JB Dixon, DG Schulze) pp. 323–366. (Soil Science Society of America: Madison, WI)

Birkeland PW (1999) 'Soils and geomorphology.' 3rd edn. (Oxford University Press: New York)

Bisdom EBA, Dekker LW, Schoute JFT (1993) Water repellency of sieve fractions from sandy soils and relationships with organic matter and soil structure. *Geoderma* **56**, 105–118. doi:10.1016/0016-7061(93)90103-R

Boyer DE, Dell JD (1980) 'Fire effects on pacific northwest soils.' USDA Forest Service, Pacific Northwest Forest and Range Experiment Station Report R6 WM 040. (Portland, OR)

D'Ascoli R, Rutigliano FA, De Pascale RA, Gentile A, Virzo De Santo A (2005) Functional diversity of the microbial community in Mediterranean maquis soils as affected by fires. *International Journal of Wildland Fire* **14**, 355–363.

Dearing JA (1994) 'Environmental magnetic susceptibility, using the Barington MS2 System.' (Chi Publishers: Kenilworth, UK)

DeBano LF (1981) 'Water repellent soils: a state-of-the-art.' USDA Forest Service, Pacific Southwest Forest and Range Experiment Station General Technical Report PSW-46. (Berkeley, CA)

DeBano LF (2000) The role of fire and soil heating on water repellency in wildland environments: a review. *Journal of Hydrology* **231–232**, 195–206. doi:10.1016/S0022-1694(00)00194-3

DeBano LF, Savage SM, Hamilton DA (1976) The transfer of heat and hydrophobic substances during burning. *Soil Science Society of America Journal* **40**, 779–782.

De Marco A, Gentile AE, Arena C, Virzo De Santo A (2005) Organic matter, nutrient content and biological activity in burned and unburned soils of a Mediterranean maquis area of southern Italy. *International Journal of Wildland Fire* **14**, 365–377.

Doerr SH, Shakesby RA, Walsh RPD (1998) Spatial variability of soil hydrophobicity in fire-prone eucalyptus and pine forests, Portugal. *Soil Science* **163**, 313–324. doi:10.1097/00010694-199804000-00006

Doerr SH, Shakesby RA, Walsh RPD (2000) Soil water repellency: its causes, characteristics, and hydro-geomorphological significance. *Earth Science Reviews* **51**, 33–65. doi:10.1016/S0012-8252(00)00011-8

Doerr SH, Blake WH, Shakesby RA, Stagnitti F, Vuurens SH, Humphreys GS, Wallbrink P (2004) Heating effects on water repellency in Australian eucalypt forest soils and their value in estimating wildfire soil temperatures. *International Journal of Wildland Fire* **13**, 157–163. doi:10.1071/WF03051

Durgin PB, Vogelsang PJ (1984) Dispersion of kaolinite by water extracts of douglas-fir ash. *Canadian Journal of Soil Science* **64**, 439–443.

Etiegni L, Campbell AG (1991) Physical and chemical characteristics of wood ash. *Bioresource Technology* **37**, 173–178. doi:10.1016/0960-8524(91)90207-Z

Evans ME, Heller F (2003) 'Environmental magnetism: principles and applications of enviromagnetics.' (Academic Press: San Diego)

Fine P, Singer MJ, LaVen R, Verosub K, Southard RJ (1989) Role of pedogenesis in distribution of magnetic susceptibility in two California chronosequences. *Geoderma* **44**, 287–306. doi:10.1016/0016-7061(89)90037-2

Giovannini GS, Lucchesi S (1983) Effect of fire on hydrophobic and cementing substances of soil aggregates. *Soil Science* **136**, 231–236.

Guerrero C, Mataix-Solera J, Gómez I, García-Orenes F, Jordán MM (2005) Microbial recolonization and chemical changes in a soil heated at different temperatures. *International Journal of Wildland Fire* **14**, 385–400.

Harden JW, Matti JC (1989) Holocene and late Pleistocene slip rates on the San Andreas fault in Yucaipa, California, using displaced alluvial-fan deposits and soil chronology. *Geological Society of America Bulletin* **101**, 1107–1117. doi:10.1130/0016-7606(1989)101<1107:HALPSR>2.3.CO;2

Hart SC, Firestone MK, Paul EA (1992) Decomposition and nutrient dynamics of ponderosa pine needles in a Mediterranean-type climate. *Canadian Journal of Forest Research* **22**, 306–314.

Kendrick KJ, McFadden LD (1996) Comparison and contrast of processes of soil formation in the San Timoteo badlands with chronosequences in California. *Quaternary Research* **46**, 149–160. doi:10.1006/QRES.1996.0055

Ketterings QM, Bigham JM (2000) Soil color as an indicator of slash-and-burn fire severity and soil fertility in Sumatra, Indonesia. *Soil Science Society of America Journal* **64**, 1826–1833.

Ketterings QM, Bigham JM, Laperche V (2000) Changes in soil mineralogy and texture caused by slash-and-burn fires in Sumatra, Indonesia. *Soil Science Society of America Journal* **64**, 1108–1117.

Kinney A (1887) Report on the forests of the counties of Los Angeles, San Bernardino, and San Diego, California. In 'First biennial report of the California State Board of Forestry, 1885–86'. (California State Board of Forestry: Sacramento, CA)

Loeppert RH, Suarez DL (1996) Carbonate and gypsum. In 'Methods of soil analysis. Part 3'. (Ed. DL Sparks) pp. 437–474. (Soil Science Society of America: Madison, WI)

McFadden LD, Hendricks DM (1985) Changes in the content and composition of pedogenic iron oxyhydroxides in a chronosequence of soil in southern California. *Quaternary Research* **23**, 189–204. doi:10.1016/0033-5894(85)90028-6

McFadden LD, Weldon RJ (1987) Rates and processes of soil development on Quaternary terraces in Cajon Pass, California. *Geological Society of America Bulletin* **98**, 280–293. doi:10.1130/0016-7606(1987)98<280:RAPOSD>2.0.CO;2

Minnich RA (1986) Snow levels and amounts in the mountains of southern California. *Journal of Hydrology* **89**, 37–58. doi:10.1016/0022-1694(86)90141-1

Minnich RA (1987) Fire behavior in southern California chaparral before fire control: the Mount Wilson burns at the turn of the century. *Annals of the American Association of Geographers* **77**, 599–618. doi:10.1111/J.1467-8306.1987.TB00183.X

Minnich RA (1988) The biogeography of fire in the San Bernardino Mountains of California: a historical survey. *University of California Publications in Geography* **28**, 1–121.

Minnich RA (1999) Vegetation, fire regimes, and forest dynamics. In 'Oxidant air pollution impacts in the montane forests of southern California: a case study of the San Bernardino Mountains'. (Eds PR Miller, JR McBride) pp. 44–78. (Springer-Verlag: New York)

Minnich RA, Chou YH (1997) Wildland fire patch dynamics in the chaparral of southern California and northern Baja California. *International Journal of Wildland Fire* **7**, 221–248.

Minnich RA, Everett RG (2001) Conifer tree distributions in southern California. *Madrono* **48**, 177–197.

Minnich RA, Barbour MG, Burk JH, Fernoe R (1995) Sixty years of change in conifer forest of the San Bernardino Mountains, California. *Conservation Biology* **9**, 902–914. doi:10.1046/J.1523-1739.1995.09040902.X

Minnich RA, Barbour MG, Burk JH, Sosa-Ramirez J (2000) Californian mixed-conifer forests under unmanaged fire-regimes in the Sierra San Pedro Martír, Baja California, Mexico. *Journal of Biogeography* **27**, 105–129. doi:10.1046/J.1365-2699.2000.00368.X

Mullins CE (1977) Magnetic susceptibility of the soil and its significance in soil science—a review. *Journal of Soil Science* **28**, 223–246.

Nelson DW, Sommers LE (1996) Total carbon, organic carbon, and organic matter. In 'Methods of soil analysis. Part 3'. (Ed. DL Sparks) pp. 961–1010. (Soil Science Society of America: Madison, WI)

Savage SM (1974) Mechanism of fire-induced water repellency in soil. *Soil Science Society of America Proceedings* **38**, 652–657.

Savage SM, Osborn J, Letey J, Heaton C (1972) Substances contributing to fire-induced water repellency in soils. *Soil Science Society of America Proceedings* **36**, 674–678.

Scheinost AC, Schwertmann U (1999) Color identification of iron oxides and hydroxysulfates: use and limitations. *Soil Science Society of America Journal* **63**, 1463–1471.

Schoeneberger PJ, Wysocki DA, Benham EC, Broderson WD (2002) 'Fieldbook for describing and sampling soils, version 2.0.' (USDA Natural Resources Conservation Service, National Soil Survey Center: Lincoln, NE)

Schwertmann U (1988) Occurrence and formation of iron oxides in various pedoenvironments. In 'Iron in soils and clay minerals'. (Eds JW Stucki, BA Goodman, U Schwertmann) pp. 267–308. NATO Advanced Science Institutes Series C, Mathematical and Physical Sciences Vol. 207. (D Reidel Publishing Company: Dordrecht)

Schwertmann U (1993) Relations between iron oxides, soil color, and soil formation. In 'Soil color'. (Eds JM Bigham, EJ Ciolkosc) pp. 51–69. (Soil Science Society of America: Madison, WI)

Schwertmann U, Fechter H (1984) The influence of aluminum on iron oxides: xi. Aluminum-substituted maghemite in soils and its formation. *Soil Science Society of America Journal* **48**, 1462–1463.

Schwertmann U, Taylor RM (1989) Iron oxides. In 'Minerals in soil environments'. 2nd edn. (Eds JB Dixon, SB Weed) pp. 379–438. (Soil Science Society of America: Madison, WI)

Sertsu SM, Sanchez PA (1978) Effects of heating on some changes in soil properties in relation to an Ethiopian land management practice. *Soil Science Society of America Journal* **42**, 940–944.

Singer MJ, Verosub KL, Fine P, TenPas J (1996) A conceptual model for the enhancement of magnetic susceptibility in soils. *Quaternary International* **34–36**, 243–248. doi:10.1016/1040-6182(95)00089-5

Soil Conservation Service (1984) 'Procedures for collecting soil samples and methods of soil analysis for soil survey.' USDA Soil Conservation Service, Soil Survey Investigation Report No. 1. (US Government Printing Office: Washington, DC)

Soil Survey Staff (1999) 'Keys to soil taxonomy.' 8th edn. (USDA Soil Conservation Service, Pocahontas Press: Blacksburg, VA)

St John TV, Rundel PW (1976) The role of fire as a mineralizing agent in a Sierran coniferous forest. *Oecologia* **25**, 35–45. doi:10.1007/BF00345032

Stanjek H (1987) The formation of maghemite and hematite from lepidocrocite and goethite in a Cambisol from Corsica, France. *Zeitschrift für Pflanzenernährung und Bodenkunde* **150**, 314–318.

Stephens SL (2004) Fuel loads, snag abundance, and snag recruitment in an unmanaged Jeffrey pine-mixed conifer forest in northwestern Mexico. *Forest Ecology and Management* **199**, 103–113.

Stephenson JR, Calcarone GM (1999) 'Southern California mountains and foothills assessment: habitat and species conservation issues.' USDA Forest Service, Pacific Southwest Research Station General Technical Report PSW-172. (Albany, CA)

Stephenson NL (1998) Actual evapotranspiration and deficit: biologically meaningful correlates of vegetation distribution across spatial scales. *Journal of Biogeography* **25**, 855–870. doi:10.1046/J.1365-2699.1998.00233.X

Stohlgren TJ (1988) Litter dynamics in two Sierran mixed conifer forests, I: litter fall and decomposition rates. *Canadian Journal of Forest Research* **18**, 1127–1135.

Torrent J, Barrón V (1993) Laboratory measurement of soil color: theory and practice. In 'Soil color'. (Eds JM Bigham, EJ Ciolkolz) pp. 21–33. SSSA Special Publication No. 31. (Soil Science Society of America: Madison, WI)

Torrent J, Schwertmann U, Fechter H, Alferez F (1983) Quantitative relationships between soil color and hematite content. *Soil Science* **136**, 354–358.

Ulery AL, Graham RC (1993) Forest fire effects on soil color and texture. *Soil Science Society of America Journal* **57**, 135–140.

Ulery AL, Graham RC, Amrhein C (1993) Wood-ash composition and soil pH following intense burning. *Soil Science* **156**, 358–364.

Ulery AL, Graham RC, Bowen LH (1996) Forest fire effects on soil phyllosilicates in California. *Soil Science Society of America Journal* **60**, 309–315.